*Exploration Geophysics (1998) **29**, 609-614*

The calculation of magnetic components and moments from TMI: A case study from the Tuckers igneous complex, Queensland

Phillip W. Schmidt
CSIRO Exploration and Mining,
North Ryde, NSW, Australia 2113
Phone: (02) 9490 8873
Fax: (02) 9490 8874
Email: p.schmidt@syd.dem.csiro.au

David A. Clark
CSIRO Exploration and Mining,
North Ryde, NSW, Australia 2113
Phone: (02) 9490 8872
Fax: (02) 9490 8874
Email: d.clark@syd.dem.csiro.au

ABSTRACT

This paper re-examines some largely forgotten methods that are eminently adaptable to modern computing environments. The methods were originally formulated before the advent of electronic computers and do not appear to have been fully developed, or given the attention they deserve. It is apparent that if an anomaly is small with respect to the geomagnetic field, which is usual, components of the anomaly can be derived from total magnetic intensity observations, or indeed, from any other component irrespective of its direction. Furthermore, for an isolated anomaly, integrals of first order moments of the components yield information such as the direction and magnitude of the total anomalous magnetic moment of the source. Improvements to the calculation of components are proposed that, i) compensate for the finite nature of survey areas, and ii) correct for the departure from a true potential field of total magnetic intensity anomalies.

Examples of the application of the methods are derived from a survey flown by Aerodata over the Tuckers Range area of north Queensland. This survey was chosen because the magnetic properties of the lithologies giving rise to the magnetic anomalies have been thoroughly studied. The selected areas include the north margin and an outlier, which contain many anomalies showing effects of magnetic remanence of reverse polarity. The results of the methods used herein agree well with those expected from the measured magnetic properties and magnetic modelling. The calculation of the total moment of the north margin yielded a declination of 35.8° and an inclination of 39.0°. A comparison with the measured properties shows that the reverse remanence of the overprint zone appears to account for about 70% of the total anomaly over the north margin. Similarly, the outlier yielded a declination of 13.7° and an inclination of 4.5°. Over the outlier the overprinted zone appears to account for about 50% of the magnetic anomaly. It seems that magnetic interpretation could be significantly enhanced by developing these methods to their full potential and incorporating them in commercial packages.

Keywords: magnetic interpretation, magnetic moments, magnetic components, Fourier filters, magnetisation, remanence

INTRODUCTION

The frequency or wave number domain, is an extremely useful environment for the manipulation of potential field data. Familiar examples of the use of this domain are upward/downward continuation and reduction-to-pole (RTP). It is not as well known, however, that any component of the anomalous field can be calculated from any other component using the same methods. Furthermore, if the size of the anomalous source is finite, well covered and adequately sampled by the survey, the components of the anomalous field enable the calculation of the direction of the total anomalous magnetisation. This anomalous magnetisation includes magnetic remanence and anisotropy effects such as mesoscopic anisotropy of magnetic susceptibility (AMS) and self-demagnetisation (macroscopic AMS). This paper explores these ideas using case studies to illustrate various points.

THEORY

Vestine and Davids (1945) were the first to suggest that three orthogonal components of a potential field could be derived from the knowledge of a single component, along any fixed direction, over a surface that lies above all sources. Hughes and Pondrom (1947) developed a method to calculate vertical and horizontal anomalies from total magnetic intensity (TMI) data (measured by then recently developed proton magnetometers) so the data could be compared more easily with older fluxgate data.

Lourenco and Morrison (1973) built on these concepts using the recently devised FFT and showed that computer power at that time could handle 32×32 grids and reproduce synthetic data with acceptable accuracy. Here we present examples of these techniques using high resolution survey data. The quality of modern surveys is sufficiently high that these techniques should become standard options available in all exploration offices.

Components of the anomalous magnetic field arising from subsurface sources are spatial derivatives of a scalar potential that satisfies Laplace's equation. Thus magnetic field components also obey Laplace's equation and are themselves potential fields. It follows from potential field theory that any magnetic field component can be derived from the measurement of another component, given sufficiently dense sampling. In most areas magnetic anomalies are small perturbations of the regional geomagnetic field. In that case the total magnetic intensity (TMI) closely approximates the projection of the anomalous field vector onto the regional geomagnetic field direction and the TMI behaves as a potential field. It is therefore possible to derive all the magnetic components from the TMI (e.g. Blakely, 1995, p.342-343), provided the anomalies are small compared to the geomagnetic field.

The Fourier transform of the total-field anomaly caused by magnetisation $M(x,y,z)$ is given by Blakely (1995) as:

$$\Im[\Delta T] = 2\pi \; C_m \Theta_m \Theta_f |k| e^{|k| z_0} \int_{z_0}^{\infty} e^{-|k| z'} \Im[M(z')] dz' \qquad (1)$$

where $\Im[M(z')]$ denotes the Fourier transform of the magnetisation of a horizontal plane through the body at depth z', z_0 is the observation height and k is the wave number ($=2\pi/\lambda$) and $C_m = 1$ in the cgs system and $\mu_0/4\pi$ ($=10^{-7}$) in the SI system.

The parameters Θ_m and Θ_f are given by:

$$\Theta_m = m_z + i\frac{m_x k_x + m_y k_y}{|k|} \tag{2}$$

$$\Theta_f = f_z + i\frac{f_x k_x + f_y k_y}{|k|} \tag{3}$$

where $m = (m_x, m_y, m_z)$ and $f = (f_x, f_y, f_z)$ are unit vectors in the direction of the magnetisation and ambient field respectively.

The form of a magnetic anomaly changes for different magnetisations, $m' = (m'_x, m'_y, m'_z)$ or different ambient magnetic fields, $f' = (f'_x, f'_y, f'_z)$.

The transformed anomaly can be described by:

$$\Im[\Delta T] = 2\pi\ C_m \Theta'_m \Theta'_f |k| e^{|k|z_0} \int_{z_0}^{\infty} e^{-|k|z'} \Im[M(z')]\, dz' \tag{4}$$

where the parameters Θ'_m and Θ'_f given by:

$$\Theta'_m = m'_z + i\frac{m'_x k_x + m'_y k_y}{|k|}, \tag{5}$$

$$\Theta'_f = f'_z + i\frac{f'_x k_x + f'_y k_y}{|k|}. \tag{6}$$

Thus the transformed anomaly is related to the observed anomaly by,

$$\Im[\Delta T_t] = \Im[\Delta T]\Im[\Psi_t] \tag{7}$$

where the filter is,

$$\Im[\Psi_t] = \frac{\Theta'_m \Theta'_f}{\Theta_m \Theta_f}. \tag{8}$$

Component Filtering

To determine the vertical component (ΔZ) we require that $\Theta'_f = f_z = 1$. The corresponding x and y direction cosines are set to zero, yielding the anomaly as it would appear if only the vertical component was measured. The magnetisation factor $\Theta'_m = \Theta_m$ since the magnetisation remains the same (note for RTP the vertical direction cosine of the magnetisation is also set to unity).

The required filter is therefore:

$$\Im[\Psi_t] = \frac{1}{\Theta_f} = \frac{|k|}{|k| f_z + i\left(k_x f_x + k_y f_y\right)}, \qquad |k| \neq 0 \tag{9}$$

Similar expressions can be derived for the horizontal components.

Integrals of Components and Moments

Helbig (1963) pointed out that integrals of anomaly components over an infinite plane are zero. Therefore, if integrations are taken over a sufficiently large area,

$$\iint \Delta T_x\, dxdy \equiv 0 \tag{10}$$

$$\iint \Delta T_y\, dxdy \equiv 0 \tag{11}$$

$$\iint \Delta T_z\, dxdy \equiv 0 \tag{12}$$

These equations can be used to adjust the TMI base level so that the TMI averages to zero and then to check that the grid of calculated components extends to a sufficient distance with respect to the lateral extent and depth of the source. Provided that these conditions are satisfied, the integrals of moments of the components have physical significance.

Moments of components are defined by integrals over the xy-plane of terms like $x_i \Delta T_j (i,j = x,y,z)$. Various moments of anomalous components are related to the magnetic moments of the source (M_t). Thus, the integral over an infinite planar surface of an anomalous component in any direction parallel to the surface yields the magnetic moment of the source perpendicular to that surface. Given that observations are available over a sufficiently large area with respect to the size of the source, this relationship is independent of the observation height, z. Following Helbig (1963) the relevant integrals are:

$$M_x^x = \iint x\ \Delta X\ dxdy = 2\pi f_z M \tag{13}$$

$$M_z^x = \iint x\ \Delta Z\ dxdy = 2\pi f_x M \tag{14}$$

$$M_z^y = \iint y\ \Delta Z\ dxdy = 2\pi f_y M \tag{15}$$

A fourth integral may be used as a check, or to reduce noise. From symmetry it is clear that both x and y share the same relationship to z, therefore:

$$M_y^y = \iint y\ \Delta Y\ dxdy = 2\pi f_z M \tag{16}$$

A parameter can be devised to estimate the accuracy of the determination of the components through examining the normalised absolute difference,

$$\Delta\Sigma = |M'_x - M'_y| / \sqrt{M'^2_x + M'^2_z + M'^2_z} \tag{17}$$

Helbig (1963) also discusses higher moments of the type $x_i\, x_j \Delta T_j (i,j = x,y,z)$ and suggested that their integrals are related to the centres of various magnetic components, analogous to the centre of mass in the gravitational case. However, it can be shown that some of the integrals of these second moments do not converge, and cannot in general be used for such an analysis.

TMI Approximation of Potential Field Anomalies

The measured TMI is an approximation of the potential field anomaly because it is the magnitude of the vector sum of the ambient geomagnetic field and the local anomalous field (e.g. see Blakely, 1995, p.178). In the terminology of Emerson et al. (1985), the measured total field anomaly (ΔB_m) can be converted by an iterative process to the theoretical anomalous component (ΔB_t) in the direction of the field, which is a true potential field. Such a procedure allows the calculation of vector anomalies and their moments even in areas of intense anomalies that significantly perturb the geomagnetic field. Results from potential field theory that constrain relationships between component anomalies and their derivatives can also be exploited. These relationships can improve interpolation of component anomalies between survey lines and improve calculation of components and their derivatives, moments and the 3D configuration of field lines.

Compensation for Far-Field Part of Anomalies

As shown above, integrating to obtain the moments of the components enables the magnetisation direction and the magnetic moment of a compact source to be derived. Reduction to the pole may then be performed with the *a priori* knowledge of the appropriate magnetisation direction. Since integration can only be performed over a finite area, the magnetic moment has to be corrected for the missing contribution of components that are either outside the survey area or are contaminated by neighbouring anomalies. An iterative procedure, that successively recalculates the far-field anomaly components using the last estimate of the dipole moment, enables convergence to the correct total moment as though the survey covered an infinite area. Nevertheless, as shown in Table 1, the direction of the moment is fairly robust, only the magnitude of the moment is significantly sensitive to the grid area. Thus for a point dipole at 200 m depth about 4% of the anomaly lies at distances greater than 6 km. It is noteworthy that the correction percentages of the total moment (10^6 Am^2 = 10^9 Gcm^3) as listed in Table 1 are independent of the direction of the moment.

Table 1. Far-field Compensation Necessary for a 10^6 Am^2 (10^9 Gcm^3) Dipole Moment†.

Grid (m×m)	Dec (°)	Inc (°)	Moment (×10^6 Am^2)	% compensation
1600×1600	333	-44	0.625	27
3200×3200	331	-45	0.834	17
6400×6400	331	-45	0.918	8
12800×12800	330	-45	0.961	4

† dipole source at 200m depth (Emerson et al., 1985, p.25)

EXAMPLE USING TUCKERS IGNEOUS COMPLEX, NORTH QLD

The Permian Tuckers Igneous Complex (TIC) is a T-shaped feature in outcrop plan, with a NE-axis of 13.5 km, oriented parallel to the Leyshon-Tuckers Corridor, and a SE-oriented axis, ~5 km in length. A small outlier occurs SE of the main complex, 1.5 km N of Hadleigh Castle. Detailed mapping of the complex was carried out by Simon Beams in 1994, as part of AMIRA project P425.

Magnetic Petrophysics of the TIC

The magnetic image over the TIC shown in Figure 1 clearly discloses the margins of the intrusive complex. Petrophysical studies (Lackie et al., 1992; Clark, 1996) have shown that there is a distinct zoning of magnetic properties around the complex, which is reflected in the image. Due to secondary magnetite, the metasomatised aureole around the complex has a somewhat higher susceptibility than the unaltered equivalent rocks of the Heathfield West Tonalite host. Igneous phases of the complex are characterised by a primary remanence directed steeply down (reverse polarity), typical of rocks of Permian age. Pyroxene and biotite hornfels zones, which are up to a kilometre wide in places,

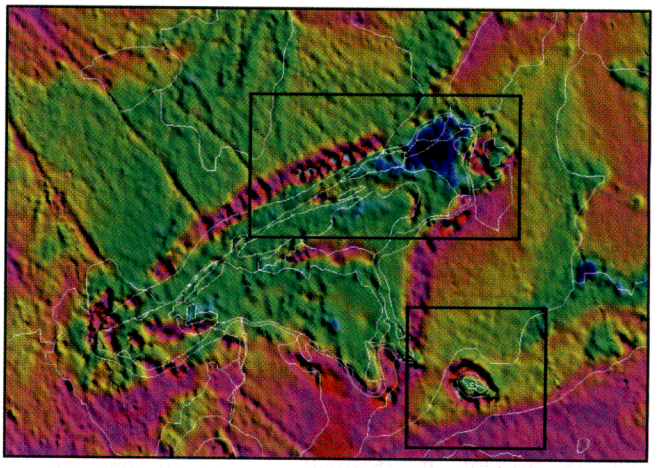

Figure 1. Reduced to Pole image of the Aerodata survey of the Tuckers Range area. Mapped geological boundaries are also shown as are the areas selected for analysis herein. The northernmost area is referred to as the North Margin, while the other area is referred to as the Outlier.

also exhibit this steep reverse polarity remanence. This remanence is ubiquitous throughout and around the margins of the complex, although it is invariably partially overprinted by lower stability normal polarity remanence so that the resultant remanent intensity is reduced by the cancelling effects of the opposite polarities. The hornfelsed host rocks and the igneous intrusion have relatively low Koenigsberger ratios. The TIC intrudes moderately magnetic Silurian tonalites and minor weakly magnetic Ordovician granites of the Ravenswood batholith. The susceptibility of the tonalite host rocks, although lower than that of the TIC, is nevertheless quite high and the most prominent magnetic signatures largely reflect contrasts in remanent magnetisation, rather than the susceptibility contrast between the TIC and the host rocks.

Immediately beyond the hornfels zone, the remanence of the Heathfield West Tonalite host is still heavily overprinted by the complex although the tonalite is not chemically altered. This overprinting is of thermal origin and is detectable up to 0.5-1 km outside the boundary of the hornfels zone, i.e. up to 1.5 km from the intrusion itself. The remanence carried by this thermally overprinted zone produces the distinct magnetic lows that surround the hornfels zone. At distances greater than 1.5-2 km from the complex, the tonalite shows no signs of the overprinting.

Average susceptibilities and natural remanent magnetisations for the various lithologies, estimated from sample measurements and confirmed by detailed modelling of magnetic profiles over the TIC, are listed in Table 2. The TIC itself is remanently magnetised shallowly to the north. Both the pyroxene and biotite hornfels zones have remanence directions to the northeast. The thermally reset zone of the host is magnetised steeply downward to the northeast while the unaffected host is remanently magnetised shallowly to the northwest. Each of these total

Table 2. Average Magnetic Properties.

Lithology	Susceptibility SI (μG/Oe)	Remanence Dirn. Dec (°)	Inc (°)	Remanence Intensity (mAm^{-1} = μG)	Koenigsberger ratio Q
TIC	0.0540 (4300)	357	-3	660	0.31
Px hornfels	0.0628 (5000)	53	+15	360	0.14
Bi hornfels	0.0535 (4260)	54	-39	700	0.33
Thermal zone	0.0314 (2500)	31	+67	1500	1.20
Host rock	0.0302 (2400)	340	-25	190	0.16

NRMs is explicable in terms of combinations of remanences acquired either in the Silurian (west-northwest with shallow upward inclination), the Permian (steep down to the south) or recently (moderate upward inclination to the north). The most intensely magnetised zone is the thermally overprinted zone which has an intensity of ~1500 mAm^{-1} (1500 μG). The magnetic anomaly rimming the TIC is therefore complex, comprising a narrow high arising from the higher susceptibility of the secondary magnetite-bearing hornfels, inward of a broader magnetic low associated with the thermally overprinted zone, which has a reversed Permian remanent magnetisation.

Components and Moment Calculations

Two areas were selected (Figure 1) for analysis using the theory outlined above which include contributions from the TIC, the hornfels, the thermally overprinted zone and the unaffected tonalite host. The TMI data extracted from the survey (Figure 1) and the vector components calculated are shown in Figures 2 and 3. Near the centres of both areas the components are dominated by the reverse magnetisation of the thermally reset zone. This is best seen in the plots showing the east and the vertical components plotted together, where downward pointing arrows represent the anomalous field that is partially cancelling the geomagnetic field, causing the magnetic lows that characterise the thermally overprinted zone.

RESULTS

Magnetic petrophysics has established the average magnetic properties for the major lithologies as listed in Table 2. The magnetic properties of the Tuckers Igneous Complex, the hornfels zones and the host rocks are dominated by induced magnetisation, with Koenigsberger ratios << 1, while the magnetic properties of the thermally reset zone are dominated by remanent magnetisation with $Q > 1$. The properties allow resultant magnetisations to be calculated, which are listed in Table 3. The magnetic anomalies arise from magnetisation contrasts, therefore where the background magnetisation is non-zero, as is the case here, the magnetisation contrasts are the relevant parameters for modelling. The magnetisation contrasts between the major lithologies and the host rocks are given in Table 4.

Table 3. Resultant Magnetisations.

Lithology	Magnetisation Dirn.		Magnetisation
	Dec (°)	Inc (°)	(mAm^{-1} = μG)
TIC	356	-40	2650
Px hornfels	7	-44	2640
Bi hornfels	12	-49	2990
Thermal zone	11	+30	1780
Host rock	355	-47	1360

Table 4. Magnetisation Contrasts with Host Rock.

Lithology	Magnetisation Contrast Dirn.		Magnetisation Contrast Magnitude
	Dec (°)	Inc (°)	(mAm^{-1} = μG)
TIC	357	-33	1310
Px hornfels	18	-40	1310
Bi hornfels	26	-49	1680
Thermal zone	32	+70	2010
Host rock	–	–	0

The measured magnetisation contrast between the hornfels zones and the host rocks is directed north-northeast with moderate negative (upward) inclination, whereas the

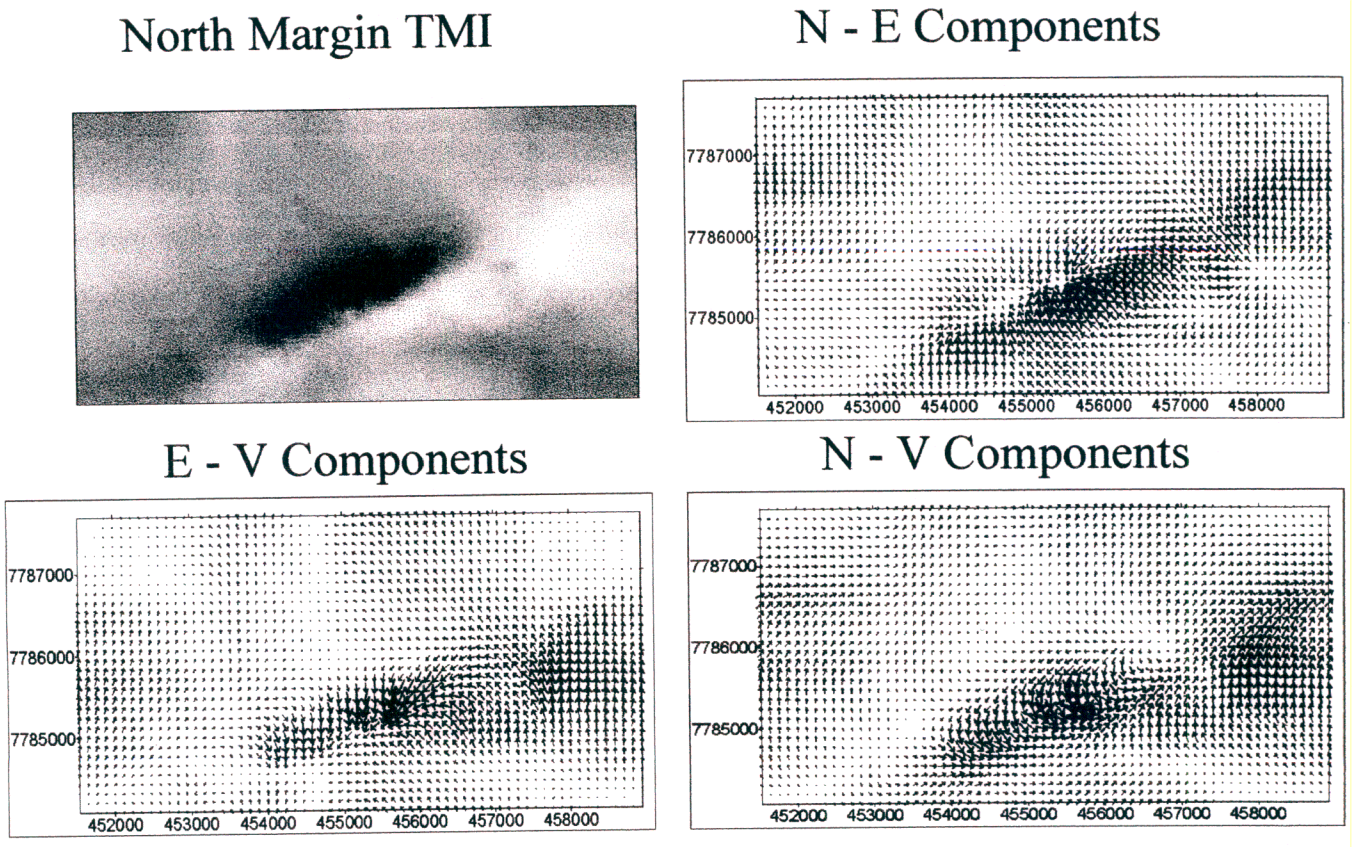

Figure 2. Composite showing a grey-scale image of part of the North Margin of the Tuckers Igneous Complex (TIC) and plots of components projected on to the horizontal and the NS and EW vertical planes. A 128 × 64 grid was used for calculations although a 64 × 32 grid is displayed for clarity.

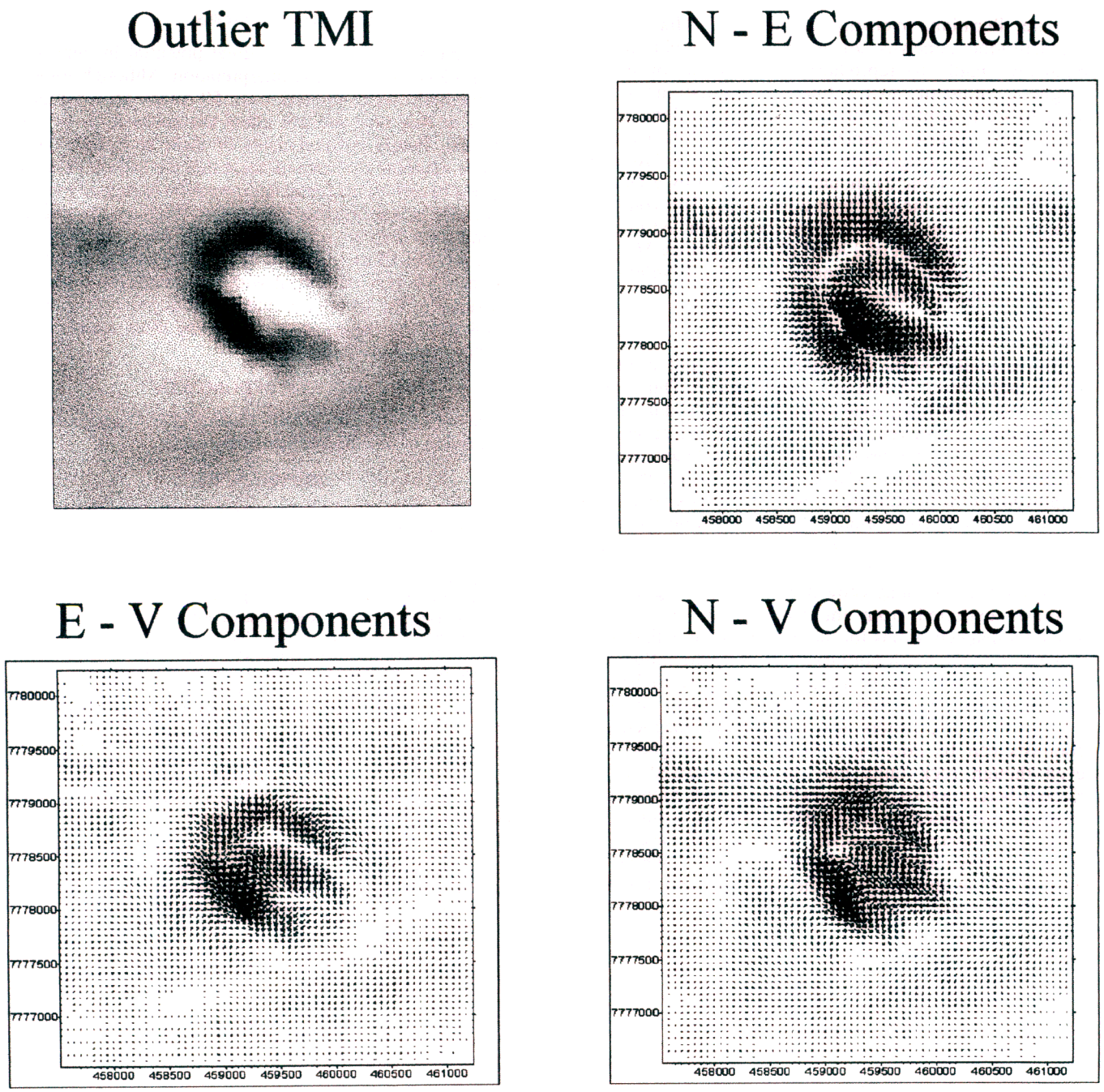

Figure 3. Composite showing a grey-scale image of part of the Outlier of the Tuckers Igneous Complex (TIC) and plots of components projected on to the horizontal and the NS and EW vertical planes.

corresponding magnetisation contrast for the thermally overprinted zone is directed steeply down to the northeast. The resultant magnetisation contrast of the combined zones is therefore predicted to be in the northeast quadrant with positive (downward) inclination. The exact inclination is difficult to determine from the measured properties only, since it depends upon the relative proportions that each lithology contributes. This is better estimated by integrating the components to calculate the total magnetisation direction.

Results of performing the integrations to determine the total magnetic moment associated with the two areas are listed in Table 5. The $\Delta\Sigma$ parameter represents the mismatch between the two independent integrals that yield the vertical component (equations 13 and 16), as a percentage of the square root of the sum of squares of all the integrals. This gives a rough guide to the overall accuracy with which the components have been determined.

Table 5. Total Magnetic Moments for Selected Areas†

Area	$\Delta\Sigma$ (%)	Dec (°)	Inc (°)	Moment ($\times 10^9$ Am^2)
North margin	5.9	35.8	39.0	2.20
Outlier	15.5	13.7	4.5	0.779

† areas shown in Figure 1.

North Margin

The calculation of the total moment of the north margin yielded a declination of 35.8° and an inclination of 39.0°. This direction is that of the net magnetisation contrast between the major lithologies and the Heathfield West Tonalite host. The contrast is clearly dominated by that due to the overprinted zone (Table 4), which is itself dominated

by the Permian overprint remanence. That is, the magnetisation contrasts arising from susceptibilities are relatively small. To reproduce the direction of the net magnetic moment, using linear combinations of the magnetisation contrasts, the relative proportions of the normal and reverse magnetisation zones must be 1:2.5. Therefore, the magnitude of the magnetic moment, 2.2×10^9 Am^2 (Table 5) should be increased by a factor of $2.5/1.5 \approx 1.7$, for the overprint zone alone. The volume of rock in the overprint zone may be then estimated using its magnetisation contrast of 2 Am^{-1} (Table 4). Since $M = J \times v$, where M is moment, J is magnetisation and v is volume, the minimum volume is about 2×10^9 m^3.

Outlier

The calculation of the total moment of the outlier yielded a declination of 13.7°, and inclination of 4.5°. Thus, for the outlier, the overprinted zone seems to be not as dominant as it is for the north margin. Nevertheless, the direction of the moment reflects the presence of a significant Permian remanent magnetisation. Using a similar approach to that employed for the north margin, 54% of the rock volume can be attributed to the overprinted zone of the outlier. Again the volume of the overprint zone can be estimated after correcting the net magnetic moment.

These results are in agreement with the net magnetisation contrasts expected from the values listed in Table 4. The total magnetisations for the two areas are both directed downward to the north-northeast reflecting the influence of the overprint zone on the magnetisation contrast between the Heathfield West Tonalite host rocks and the other lithologies. These results also suggest that magnetisation contrasts can be dominated by remanent magnetisation, even though rock units may be characterised by low Koenigsberger ratios. Thus, calculation of moments of anomaly components yields results that are explicable in terms of magnetic properties, even in the case of the complex magnetic signature of the TIC, which has overlapped anomalies from the hornfels and thermally overprinted zones.

CONCLUSIONS

The methods outlined have great potential in improving the efficiency of magnetic interpretation. Although some of the methods were devised over 50 years ago, computer power at that time did not allow the methods to be fully explored. Future enhancements of these techniques could include mapping the lines-of-force that we believe would be of great benefit to magnetic interpretation in rugged terrains, especially in low magnetic latitudes. We have investigated several data sets in addition to those analysed here (see Schmidt and Clark, 1997) and in all instances found the results to be very consistent with rock magnetic properties measured in the laboratory and magnetic modelling. There seems to be no impediment to building these methods into standard computer packages.

ACKNOWLEDGMENTS

The authors thank World Geoscience Corporation for permission to use their aeromagnetic data.

REFERENCES

Blakely, R.J., 1995, Potential Theory in Gravity and Magnetic Applications, Cambridge University Press.

Clark, D.A., 1996, Palaeomagnetism of the Mount Leyshon Intrusive Complex, the Tuckers Igneous Complex and the Ravenswood Batholith. CSIRO Exploration and Mining Report 318R.

Emerson, D.W., Clark, D.A. and Saul, S.J., 1985, Magnetic exploration models incorporating remanence, demagnetization and anisotropy: HP41C handheld computer algorithms: Expl. Geophys., **16**, 1-122.

Helbig, K., 1963, Some integrals of magnetic anomalies and their relation to the parameters of the disturbing body: Z. Geophysik, **29**, 83-96.

Hughes, D.S. and Pondrom, W.L., 1947, Computation of vertical magnetic anomalies from total magnetic field measurements: American Union Transactions, **28**, 193-197.

Lackie, M.A., Clark, D.A. and French, D.H., 1992, A regional survey of the rock magnetic properties of the Ravenswood Igneous Complex, northeast Queensland. CSIRO Exploration and Mining Report 279R.

Lourenco, J.S. and Morrison, H.F., 1973, Vector magnetic anomalies derived from measurements of a single component of the field: Geophysics, **38**, 359-368.

Schmidt, P.W. and Clark, D.A., 1997, Directions of magnetisation and vector anomalies derived from total field surveys: Preview, **70**, 30-32.

Vestine, E.H. and Davids, N., 1945, Analysis and interpretation of geomagnetic anomalies: Terrestrial Magnetism and Atmospheric Electricity, **50**, 1-36.